



Isolation of monoclonal antibodies from anti-synthetase syndrome patients and affinity maturation by recombination of independent somatic variants

Luke Burman , Yeeting E. Chong , Sherie Duncan , Anders Klaus , Kaitlyn Rauch , Kristina Hamel , Karine Hervé , Stephanie Pfaffen , David W. Collins , Kevin Heyries , Leslie Nangle , Carl Hansen & David J. King

To cite this article: Luke Burman , Yeeting E. Chong , Sherie Duncan , Anders Klaus , Kaitlyn Rauch , Kristina Hamel , Karine Hervé , Stephanie Pfaffen , David W. Collins , Kevin Heyries , Leslie Nangle , Carl Hansen & David J. King (2020) Isolation of monoclonal antibodies from anti-synthetase syndrome patients and affinity maturation by recombination of independent somatic variants, mAbs, 12:1, 1836718, DOI: [10.1080/19420862.2020.1836718](https://doi.org/10.1080/19420862.2020.1836718)

To link to this article: <https://doi.org/10.1080/19420862.2020.1836718>



© 2020 aTyr Pharma. Published with license
by Taylor & Francis Group, LLC.



[View supplementary material](#)



Published online: 01 Nov 2020.



[Submit your article to this journal](#)



Article views: 211



[View related articles](#)



[View Crossmark data](#)

REPORT

 OPEN ACCESS 

Isolation of monoclonal antibodies from anti-synthetase syndrome patients and affinity maturation by recombination of independent somatic variants

Luke Burman^a, Yeeting E. Chong^a, Sherie Duncan^b, Anders Klaus^b, Kaitlyn Rauch^a, Kristina Hamel^a, Karine Hervé^b, Stephanie Pfaffen^b, David W. Collins^b, Kevin Heyries^b, Leslie Nangle^a, Carl Hansen^b, and David J. King^{a#}

^aDiscovery Biology, aTyr Pharma, San Diego, CA, USA; ^bAbCellera Biologics Inc., Vancouver, BC, Canada

ABSTRACT

The autoimmune disease known as Jo-1 positive anti-synthetase syndrome (ASS) is characterized by circulating antibody titers to histidyl-tRNA synthetase (HARS), which may play a role in modulating the non-canonical functions of HARS. Monoclonal antibodies to HARS were isolated by single-cell screening and sequencing from three Jo-1 positive ASS patients and shown to be of high affinity, covering diverse epitope space. The immune response was further characterized by repertoire sequencing from the most productive of the donor samples. In line with previous studies of autoimmune repertoires, these antibodies tended to have long complementarity-determining region H3 sequences with more positive-charged residues than average. Clones of interest were clustered into groups with related sequences, allowing us to observe different somatic mutations in related clones. We postulated that these had found alternate structural solutions for high affinity binding, but that mutations might be transferable between clones to further enhance binding affinity. Transfer of somatic mutations between antibodies within the same clonal group was able to enhance binding affinity in a number of cases, including beneficial transfer of a mutation from a lower affinity clone into one of higher affinity. Affinity enhancement was seen with mutation transfer both between related single-cell clones, and directly from related repertoire sequences. To our knowledge, this is the first demonstration of somatic hypermutation transfer from repertoire sequences to further mature *in vivo* derived antibodies, and represents an additional tool to aid in affinity maturation for the development of antibodies.

ARTICLE HISTORY

Received 28 May 2020
Revised 23 September 2020
Accepted 10 October 2020

KEYWORDS

Aminoacyl tRNA synthetase; antibody; autoimmune disease; bioinformatics; cellular immune response; protein evolution; repertoire; single cell

Introduction

Various approaches have been successfully applied to identify and isolate antibodies with high specificity for their target. Technologies such as hybridoma fusion, transgenic mice, and phage/yeast/mammalian display have led to the successful development of this class of therapeutics.^{1–5} While these approaches have been productive, new technological advances continue to improve our ability to probe the immune response and isolate functional antibodies. Single B cell isolation and sequencing⁶ provide a means to recover paired antibody sequences with known specificity, while high-throughput repertoire sequencing⁷ provides a broad sampling of the immune response. The use of these techniques in a complementary fashion has the potential to accelerate the development of antibody therapeutics against novel targets.

Monoclonal antibodies have been selected directly from human B cells by a number of techniques, and innovative approaches to prolong the survival of human antibody-producing cells and to recover immunoglobulin sequences directly from them have been developed.^{8–11} The ability to obtain paired immunoglobulin heavy and light chain sequences from single B cells by reverse transcription-polymerase chain reaction (RT-PCR) allows antibodies to be recovered from rare B cells.⁶ Cells with antigen-specific Ig sequences can be isolated by a number of techniques, including flow cytometry,^{12,13} microfluidics to isolate

cells followed by high-throughput sequencing,¹⁴ or bead-based screening.¹⁵

Antibody repertoire diversity is developed based on initial variable(diversity)joining (V(D)J) gene rearrangement followed by somatic hypermutation (SHM) to select for antibodies with high affinity and specificity for the target antigen. Recent advances in next-generation sequencing (NGS) and data analysis of immunoglobulin gene repertoires (Ig-seq) have enabled investigation of the natural diversity of antibodies in individual animals or humans.^{16,17} This data is leading to new insights into how immune responses are elicited and developed, for example, in response to infection and vaccination.^{18,19} This has aided studies of SHM such that maturation of antibody sequences can be understood in more detail than previous methodology allowed.

As part of this analysis, it has become apparent that SHM of antibodies can take multiple paths to improve the affinity and properties of rearranged antibody sequences, with parallel routes resulting in many related antibody sequences observed in the immune repertoire.^{20,21} The heavy chain complementarity-determining region (CDR) 3 sequence is formed at the junction of the heavy chain V, D, and J genes in an imprecise joining event in which nucleotides may be deleted or added in a non-templated fashion. As such, CDR3 sequences are often diagnostic of gene rearrangement events and may allow alternately matured antibodies to be identified that come from

CONTACT Luke Burman  lburman@atyrpharma.com  aTyr Pharma, San Diego, CA 92121

[#]Present address: Lassen Therapeutics, San Diego, CA, USA

 Supplemental data for this article can be accessed on the [publisher's website](#).

© 2020 aTyr Pharma. Published with license by Taylor & Francis Group, LLC.

This is an Open Access article distributed under the terms of the Creative Commons Attribution-NonCommercial License (<http://creativecommons.org/licenses/by-nc/4.0/>), which permits unrestricted non-commercial use, distribution, and reproduction in any medium, provided the original work is properly cited.

similar, or identical, original rearranged gene sequences. This can lead to panels of related sequences with different somatic mutations that result in different molecular solutions to the generation of high-affinity binding to a particular antigen.²²

The information contained within these different antibody sequences might allow novel recombination strategies to generate improved antibodies for high-affinity antigen binding. We sought to determine whether this was a viable route to further *in vitro* antibody maturation.

Histidyl-tRNA synthetase (HARS) is one of a number of aminoacyl-tRNA synthetases that have additional functions outside of protein synthesis, with both intracellular and extracellular non-canonical functions reported.^{22–25} Several aminoacyl-tRNA synthetases, including HARS as well as splice variants from their genes, are secreted and have potentially important roles in regulation of the immune system.^{26–29} Monoclonal antibodies to HARS are, therefore, of interest for their potential ability to regulate the immune system. The rare human autoimmune disease, Jo-1 positive anti-synthetase syndrome (ASS), is characterized by the presence of autoantibodies to HARS.³⁰ These autoantibodies remove free HARS from the circulation and are associated with individuals exhibiting activated immune pathology.²⁹ The HARS protein can be divided into three domains: 1) an N-terminal coiled-coil WHEP domain, 2) a central catalytic domain, and 3) a C-terminal anticodon binding domain (ABD). Autoantibodies have been reported to most frequently recognize epitopes within the N- or C-terminal domains.²⁶ In this study, we set out to isolate human monoclonal antibodies to HARS from Jo-1 positive individuals, and to investigate the generation of high-affinity antibodies using the information available in related sequences.

Results

Isolation of monoclonal antibody sequences from individual B cells

Peripheral blood mononuclear cells (PBMC) were collected from individuals with Jo-1 positive ASS. B cells were enriched,

and single antibody-secreting cells were isolated using AbCellera's microfluidic screening system. Single-cell isolation for antibody discovery via related approaches has been reviewed (see ref.³¹) and is widely available.

Serum from these individuals demonstrated that each one had a positive titer to HARS, including antibodies to the WHEP domain as well as other regions of the protein (data not shown). Single cells secreting antibodies specific to HARS were identified using beads coated with protein A to select for both IgG and IgA antibodies and detected with fluorescently labeled HARS. It has been reported that the N-terminal WHEP domain may be an immuno-dominant epitope in the ASS anti-HARS response,²⁶ and therefore three different recombinant HARS proteins were used for screening: Antigen 1, a full-length protein (lacking a C-terminal CIC motif to improve expression yields); Antigen 2, the isolated WHEP domain fused to maltose-binding protein (WHEP-MBP); and Antigen 3, an N-terminal WHEP deletion mutant. Antibody-secreting cells were selected based on their ability to bind full-length HARS, and further characterized by their ability to bind the WHEP domain as shown in Figure 1. WHEP domain-specific binders were defined as being able to bind full-length HARS and not the WHEP domain deletion mutant. Not all of these were able to bind to the WHEP-MBP fusion protein, likely because of an altered conformation of the WHEP domain in this protein, but also possibly due to an epitope that spanned the deletion. Unexpectedly, WHEP domain-specific binders were in the minority in these selected clones (Table 1). Cells secreting antibodies with the desired properties were recovered from the screening device, and single-cell RT-PCR followed by NGS was used to identify the corresponding paired antibody heavy and light chain sequences.

In this study, single-cell-derived antibodies were obtained from screening three donors with Jo-1 positive ASS. Due to the rarity of patients^{32,33} and the difficult logistics of timely sample delivery, the quality of each sample at screening varied drastically, resulting in only three of six samples showing antibody secretion, as well as variable single-cell recovery from each

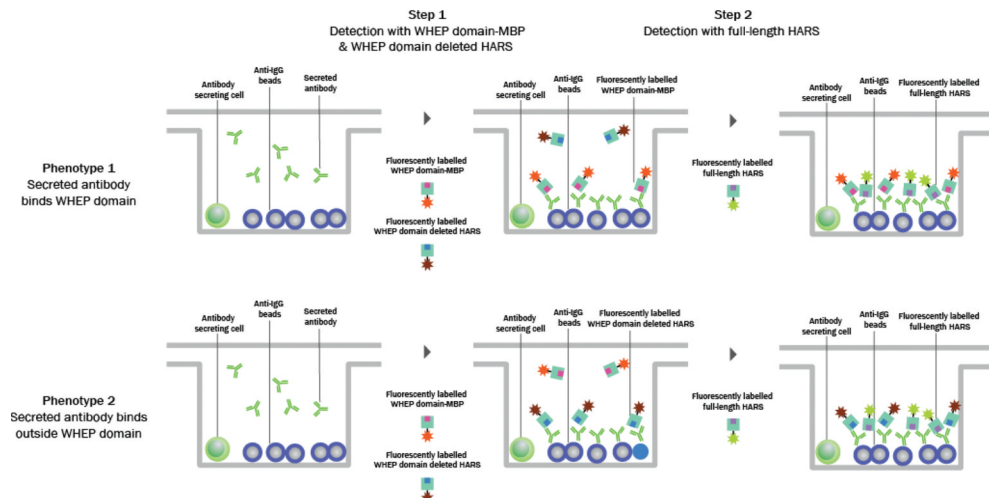


Figure 1. Assay format used for single-cell antibody discovery. A two-step screening assay was performed. In step 1, antibody-secreting cells were co-incubated with protein A beads to capture secreted antibodies and were detected using fluorescently labeled WHEP domain-MBP and WHEP domain-deleted HARS (left). In step 2, fluorescently labeled full-length HARS was added to confirm binding to the full-length protein (right). The two phenotypes observed during screening are depicted in the schematic: specificity to the WHEP domain (top panel, Phenotype 1) and specificity outside the WHEP domain of HARS (bottom panel, Phenotype 2).

Table 1. Summary of isolated clone sequences. Analysis of SHM, CDR charge, and length, was performed on all 195 light and heavy chains. Characterization of WHEP binding was as determined by the initial screening paradigm outlined in Figure 1.

Donor ID	1	2	3
Donor Age	53	67	29
Selected clones	131	4	60
WHEP-specific	16	2	3
IgG/IgA	117/14	2/2	58/2
Kappa/lambda	121/10	4/0	47/13
Most frequent germline genes used	VH3-23(54%)/VK4-1(56%)	VH3-53(50%)/VK4-1(75%)	VH3-23(33%)/VK4-1(33%)
% nt SHM (mean)	7% (HC), 4.2% (LC)	8% (HC), 1.8% (LC)	6.4% (HC), 4% (LC)
% aa SHM (mean)	11% (HC), 7.9% (LC)	11% (HC), 3.8% (LC)	10.6% (HC), 7.8% (LC)
CDRH3 length distribution	8–20 AVG 15.9aa	13–16 AVG 14.3aa	8–23 AVG 15.9aa
CDR-H3 (+) distribution	0–5 AVG 2.76	1–3 AVG 1.5	0–4 AVG 2.03
CDR-H3 (-) distribution	0–4 AVG 1.79	1–2 AVG 1.25	0–3 AVG 1.43

successful sample. A total of 574 paired heavy and light chain sequences were obtained, resulting in 195 unique pairs (Table 1 and supplementary Table 1). Of these, the majority (131) were obtained from a single individual, with only four from the second subject and 60 from the third. As expected from the detection methodology, the majority of recovered clones were IgG (177/195), and the remainder IgA (18/195), with most having kappa light chains (172/195), and four of the 23 lambda chains paired with IgA heavy chains. Within the 195 clones, there were 191 unique heavy chain sequences and 194 unique light chain sequences. Sequences were derived from a broad range of V-gene segments covering six variable heavy (VH) subgroups, four variable kappa (VK) groups, and five variable lambda (VL) groups, with a distribution of germline gene usage. The most frequently observed V genes in this data set, VH3-23 and VK4-1, were used in almost half of the sequences (47% and 50%, respectively) and were paired 31% of the time, suggesting some preferential pairing in this response. SHM of the selected antibodies was apparent, suggesting active maturation of the auto-antibody response to HARS. The number of VH-gene residues that had undergone somatic mutation ranged up to 28% with a mean of 10.9% (supplementary Table 2 and Table 1), consistent with reports of the degree of somatic mutation in responses to infection.^{34,35} By subdivision of antibodies by V-gene, J-gene, and CDRH3 or CDRL3 length, 91 heavy chain clusters and 63 light chain clusters are formed; these are arranged into 130 clonal families schematically represented by their heavy/light chain pairing, and antigen specificity (Fig. S1).

Comparison of auto-antigen specific clones to immunoglobulin repertoire in the same donor

In parallel to single-cell screening, immunoglobulin repertoire sequencing was carried out on Donor 1, from which the majority of paired chain sequences were identified. In two rounds of NGS, 5887 unique, productive heavy chain V-regions were obtained, aligning to 49 different V genes.

After initial clonal grouping by shared V gene, J gene, and CDR3 length, 38 trees were constructed that contained both repertoire and single-cell heavy chain sequences. In total, these trees contained 469 repertoire chains and 103 single-cell chains, five of which were an exact match between the two datasets. Further clustering on CDR3 distance reduced the clonal groups to 14 trees containing 20 repertoire sequences and 39 single-cell sequences. Several representative trees showing the relationship of individual isolated clones to sequences retrieved from the repertoire are shown schematically (Fig. S2). While these trees are based on V/J pairing and CDRH3 length, further characterization by CDRH3 homology forms distinct branches (subclones) and are detailed in Supplemental Table 2.

As selection of self-reactive clones from the individual is non-exhaustive, the repertoire itself likely includes many other self-reactive antibodies, both clonally related to the identified single-cell clones, and other independent antibodies for which no single-cell clone was identified. While it was possible to filter the repertoire data from single cell-related clones based on the clonal trees described above, it is impossible to remove with certainty all self-reactive clones. In this case, it was deemed most appropriate to perform the analysis against the unfiltered repertoire, with the assumption that any significance seen would be muted by the presence of the self-reactive clones within the repertoire. We compared the repertoire to all unique heavy chains recovered from the single cells of Donor 1. The collapse to unique sequences changed the values slightly as compared to Table 1.

Relative usage and pairing of VH and VJ genes for both repertoire (Figure 2a) and single-cell sequences (Figure 2b) are shown as a Sankey plot. Within the repertoire, there was a bias for pairing of IGHV3-23 withIGHJ4 (6%), but not as pronounced as that seen in single cells (48%). Percent usage of IGHV3-23 within the repertoire was 10% compared to the 54% seen within single cells. Within the single cells, usage of all IGHJ4s was 72% compared to the repertoire usage of IGHJ4 of 53%. The degree of SHM was lower in the isolated clones than in the general repertoire, with relative average nucleotide mutation frequency in the heavy chain V-gene of 7% for isolated clones and 7.9% in the repertoire (Figure 3a). This is despite the presumed extended exposure to antigen in the autoimmune patients, and the extended period of time for affinity maturation. It is possible that some of this observed difference is due to error intrinsic to NGS.³⁶ However, we followed best practices, as has been reviewed (see ref.³⁷), to mitigate NGS error, and a recent study of NGS error in Ig-seq³⁸ showed error rates that would not change our interpretation. Average CDRH3 length was slightly longer in the single-cell clones, 15.9 amino acids vs 15.2 from the repertoire (Figure 3b). An analysis of charged residues contained within CDRH3 showed that, in agreement with prior observations,³⁹ positively charged lysine and arginine residues are seen at a much higher frequency within the self-reactive clones, with an average per H3 of 1.56 in repertoire vs 2.41 in single cells (Figure 3c). In contrast, little change was seen in the presence of negatively charged aspartate and glutamate, with an average per H3 of 1.98 in repertoire vs 1.82 in single cells

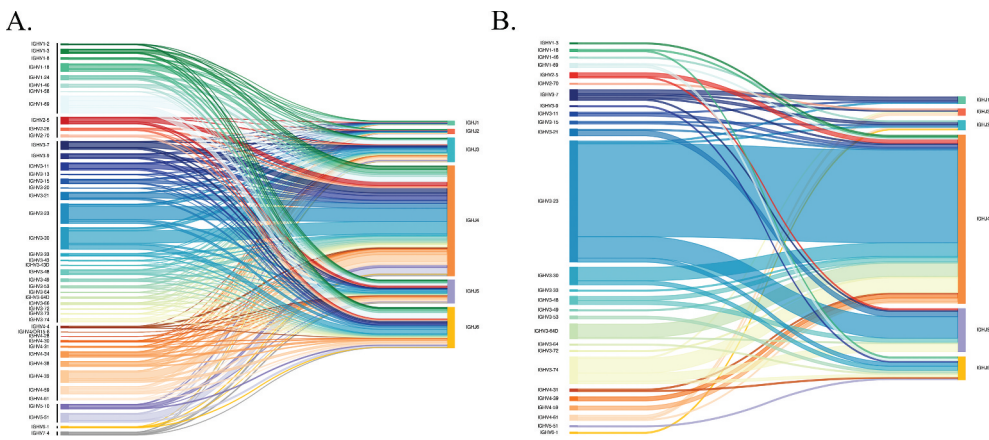


Figure 2. Frequency and pairing of V and J genes within single cell (b) and repertoire (a) heavy chains. V genes are shown on the left and J genes are shown on the right of each diagram. V/J pairing is represented by a horizontal-colored line joining the respective V and J gene. Single-cell data was collapsed to unique chains. (A) V/J gene frequency and pairing in repertoire heavy chains from Donor 1, including both self-reactive, and non-self-reactive clones. (B) V/J gene frequency and pairing in heavy chains from recovered self-reactive single-cell clones from Donor 1.

(Figure 3d). Analysis of samples from the other two Donors showed similar trends in Donor 3, while the number of recovered events from Donor 2 were too low to draw any conclusions (Figure 3a-d).

Expression and characterization of selected antibodies

Antibodies were selected for expression and characterization based on IgG sequence frequency in the dataset and degree of SHM as an indication of antibodies that had likely undergone affinity maturation, with a preference to include WHEP domain-specific binders. Sequences that potentially had certain poor developability characteristics were excluded, including those with free cysteines, N-glycosylation sites, and high likelihood deamidation or cleavage sites in CDRs (unless germline encoded). This resulted in the selection of 40 antibody sequences that were expressed and tested via biolayer interferometry (BLI) (Supplementary Table 3A). Based on V/J chain gene usage, H3 length and homology, there was some clonal overlap, with the 40 antibodies representing 28 clonotypes. In some instances, antibodies differed only in their SHM content. 35/40 were positive for binding to full-length HARS, with affinities that ranged from low nM to low pM K_D , which was also confirmed by enzyme-linked immunosorbent assay (ELISA) (Fig. S3). Of the antibodies with binding to HARS, 7/35 were demonstrated to be able to bind the WHEP domain by ELISA with his-tagged WHEP domain,²⁷ although only 4 of these bound to the WHEP-MBP fusion protein, possibly due to an altered conformation or poor accessibility of the WHEP domain when presented as a fusion protein with MBP. Five of the antibodies bound a HARS variant with a deleted catalytic domain,²⁶ but not to the WHEP, and are therefore likely to bind to the anticodon binding domain (amino acids 399–506), and the remainder are presumed to bind the central catalytic domain. A high proportion of the catalytic and anticodon domain binders had very high affinity (low pM) when screened against full-length HARS, or the WHEP-deletion mutant (20/28). As the WHEP domain is known to be disordered,⁴⁰ it is possible that the antibodies that bind in this region have lower overall affinity to the full-length protein.

Generation of high-affinity monoclonal antibodies by recombination of independent somatic variant sequences

Two WHEP domain-specific antibodies, clones 14 and 92 (Ab14 and Ab92) from Donor 1, were identified as candidates for testing SHM recombination. Ab14 was included in the initial analysis of 40 antibodies, while Ab92 was chosen as a potentially related clone. Sequence analysis of the heavy chain (Figure 4a) and light chain (Figure 4b) showed these antibodies used the same germline V-genes (IGHV3-11*06, IGKV1D-12*01) and J-genes (IGHJ4*02, IGKJ2*01). While the two antibodies share no SHM events in either the light or heavy chain V-gene at the amino acid level, they do share eight nucleotide substitutions in the heavy chain V gene (Fig. S4A, B). Sequence differences in the heavy chain were restricted to residues in CDRs and the framework (FW) 3 region that is often important for antigen binding specificity (Figure 4 and S4). In the light chain, differences were mostly in FW2 and CDR2, with one in FW3 and CDR3, respectively. The CDRH3 sequences of these two antibodies are both 11 residues in length and have five residues in common. A nucleotide alignment of the V(D)J junction shows both antibody heavy chains may have used the D-19*01 gene segment during rearrangement, while 7/13 consecutive nucleotides match within the VD non-homologous end joining (NHEJ) (Fig. S4C). By surface plasmon resonance (SPR), Ab14 had a lower affinity than Ab92 (K_D 371 nM vs 2.1 nM) (Figure 5a, b, e) even though it was more somatically mutated (10 V-gene amino acid replacements compared to 8). No additional clones in this V(D)J lineage were isolated from the repertoire sequencing, so it is impossible to elucidate their relationship further.

These antibodies were confirmed to compete with each other via indirect ELISA against full-length HARS, suggesting similar or overlapping epitopes (Fig. S5A, B). Recombination of heavy and light chains from each antibody resulted in functional binders with intermediate affinities (Fig. S6). On the basis that these antibodies may have found similar, yet independent, molecular solutions to binding, and that the sites of SHM may indicate residues of importance in the binding interface, we transferred a number of residues between antibodies, concentrating on those that were most different in charge or

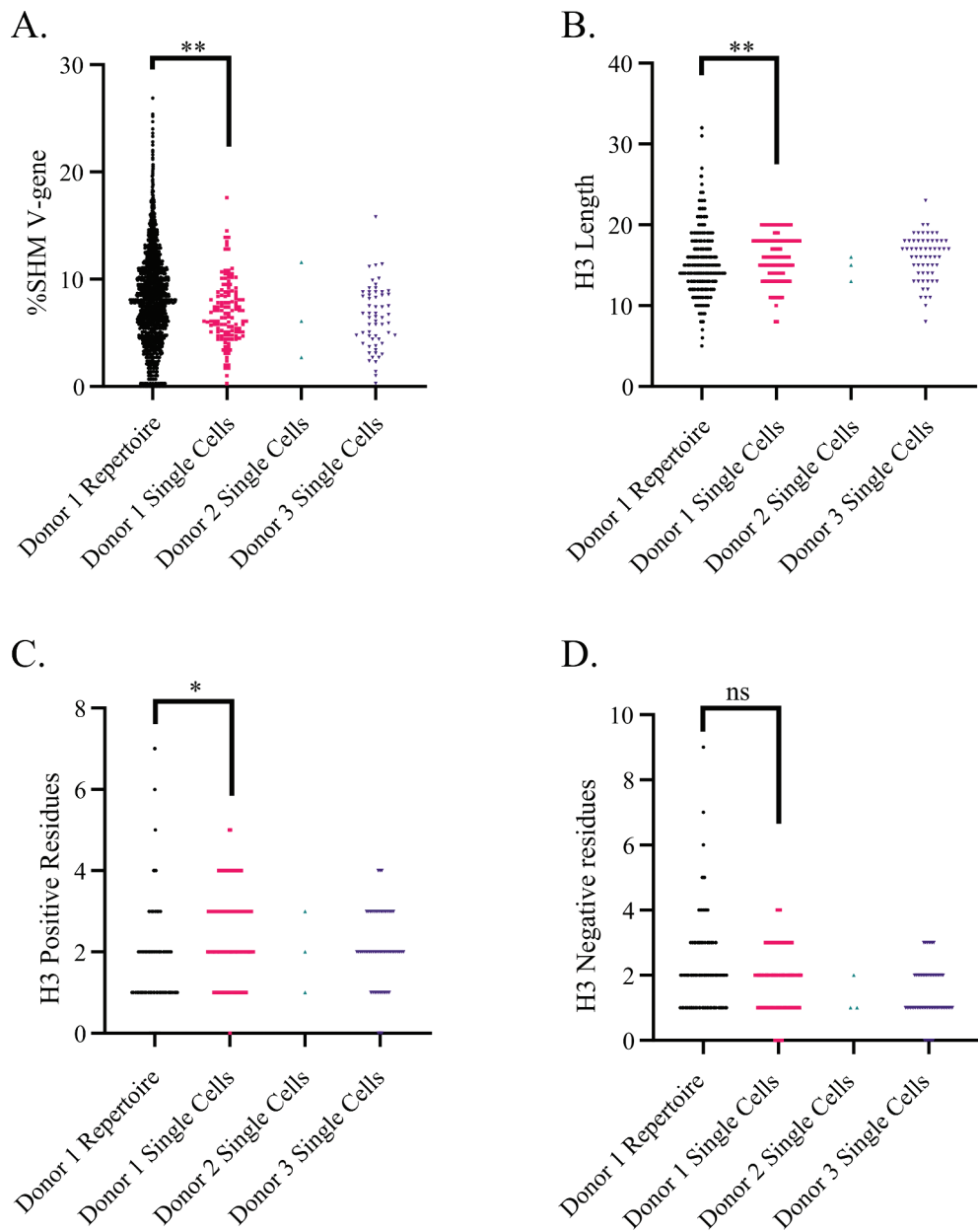


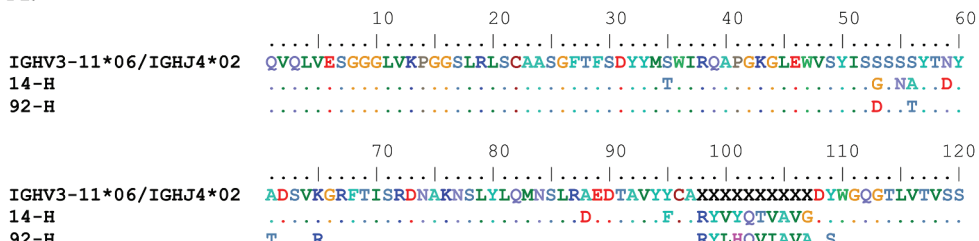
Figure 3. Comparison of heavy chain features from single cells, collapsed to unique sequences, to 5887 unique sequences recovered in the repertoire. Significance between Donor 1 repertoire and Donor 1 single cells calculated by Kolmogorov Smirnov test. * = $p < .05$, ** = $p < .005$, ns = not significant. Comparison of: (a) nucleotide SHM, (b) heavy chain CDR3 length, (c) heavy chain positive residues per CDR3 (lysine and arginine), (d) heavy chain negative residues per CDR3 (glutamate and aspartate).

hydrophobicity. We saw the greatest improvements from transfer of CDR3 residues. The most significant improvement in Ab92 affinity came from the transfer of a CDRH3 residue from Ab14 (H97Y), which resulted in a greater than 10-fold increase to a K_D of 0.19 nM (Figure 5c, e), while the reverse transfer from Ab92 to Ab14 (Y97H) resulted in a substantial loss in affinity (not shown). It was unexpected to see such a large improvement of affinity of Ab92 by transferring a substitution from a lower affinity antibody with sub-optimal binding. A transfer from Ab92 to Ab14 at residue 99 (T99V) resulted in over a 60-fold increase in affinity for Ab14 to a K_D of 5.6 nM (Figure 5d, e). Transfers in other regions had lesser impact. A transfer from light chain FW2, from Ab14 to Ab92 (Y49F) was found to increase the on-rate by twofold, but

with a loss of off-rate, and inconsistent overall affinity gain. Reversion of other SHM events in the light chain at positions 42 and 70 did not improve the affinity of Ab92, nor did those in the V-gene of the heavy chain (Figure 5f). Our principal focus was to improve the higher affinity antibody, so only limited Ab92 to Ab14 transfers were made, which we assume would be more likely to be beneficial.

While it appears obvious that the mutation transfers performed here between isolated antibody clones could also be applied to transfers from related sequences identified from repertoire sequencing, we attempted to show this directly. Based on the assembled clonal grouping, epitope mapping, and affinity testing of the set of 40 isolated antibodies, we chose four candidate molecules with varied affinity that had

A.



B.

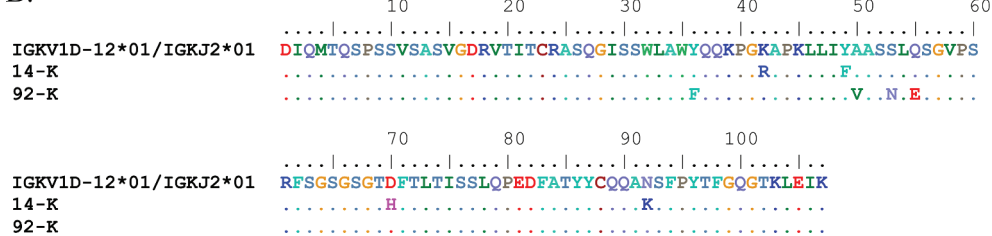


Figure 4. (a) Alignment of Ab14 and Ab92 heavy chain V region to germline sequences IGHV3-11*06 and IGHJ4*02. Identities are represented as dots, SHM substitutions are shown. V(D)J junction represented as Xs. (b) Alignment of Ab14 and Ab92 light chain V region to germline IGKV1D-12*01 and IGKJ2*01.

related heavy chain sequences in the repertoire to perform affinity maturation. Sequences were considered clonally related if they used the same V and J genes and had similar CDR3 sequences (see Methods). Two antibodies defined as anticodon binding (Ab31 and Ab54), and two catalytic domain binding antibodies (Ab62 and Ab77) were selected. Each heavy chain was paired and aligned to at least one clonally related heavy chain from the repertoire, Ab31 with rep-3352, Ab54 with rep-3401, Ab62 with rep-3497, and 3498, and Ab77 with rep-3300 and 3303 (Fig. S7A-D). While no affinity information exists for these related clones, the transfer of affinity from Ab14 to Ab92 described previously demonstrates that the affinity of the source antibody is not a limitation on its utility as a donor sequence, so we were confident that there would be valuable binding information within the matching repertoire sequences. Thirty-four mutations within CDRs or otherwise predicted to be in close proximity to the antigen were chosen for transfer from the repertoire sequences to the isolated clones, to be expressed at small scale, and screened for affinity to full-length HARS via SPR. Thirty-three of these mutations were single substitutions, with a single double substitution containing a reversion to germline to avoid a glycosylation site.

Within the set of substitutions chosen, we found six possibly beneficial substitutions (Figure 6 and Supplementary Table 3B). Two mutations, Ab62-S74P and Ab62-D100dG, had unmeasurable off rates in this experiment, and were artificially limited to $1 \times 10^{-5} \text{ s}^{-1}$ for the purposes of comparison. These two mutations, and a T28I mutation in Ab77, showed benefits of approximately threefold. Other beneficial substitutions in Ab77 and Ab31 improved affinities twofold or less. While the affinity benefit of individual substitutions was modest, there is likely sufficient information to mature Ab62 at least an order of magnitude if improving mutations were recombined. Mutations showing benefit covered various regions, including CDRs, FW3, and the N terminus of the heavy chain. Interestingly, beneficial mutations were found in regions outside the CDRs that would not typically be included in targeted mutagenesis.

Discussion

This study analyzed the immune response and antibodies isolated from three human donors with Jo-1 positive ASS. Although only a limited fraction of the anti-HARS immune response was analyzed in each PBMC sample, it was apparent that anti-HARS antibody sequences isolated were diverse and affinity matured toward the HARS auto-antigen. Previous studies on auto-antibody development have suggested that self-reactive antibodies from early B cells, which are usually removed through checkpoints in development, tend to have long and highly positively charged heavy chain CDR3 regions.³⁹ Highly positively charged CDR sequences have also been linked to antibody self-association,⁴¹ consequently, antibodies screened/isolated from autoimmune patients might require additional optimization should they be used to generate therapeutic candidates. Here, we observed increased positive charge and sequence length within the CDRH3 region of self-reactive clones isolated from single cells compared to repertoire sequences from the same individual. It is unknown if this is an effect of naive B-cells with charged CDRs escaping selective mechanisms, or antigen-driven selection of specific characteristics; a more extensive analysis of matured self-reactive antibodies to various antigens would need to be performed to draw broader conclusions.

It has been proposed that there is rarely enough selective pressure *in vivo* to drive affinity maturation of antibodies to extremely high affinities, as antibody K_D values in the nM-pM range are usually sufficient to clear the relevant antigen.^{42,43} For example, observations in humans hyper-vaccinated with tetanus toxoid have shown that antibodies can reach maximum K_D values between 0.34–1.0 nM.⁴⁴ In contrast, clones recovered in this study were frequently measured with low pM K_D s, with several exhibiting off-rates too low to measure accurately. In this case, we have no information as to the onset, and thus the duration, of the immune response to HARS in each individual; however, auto-antibodies have likely matured over

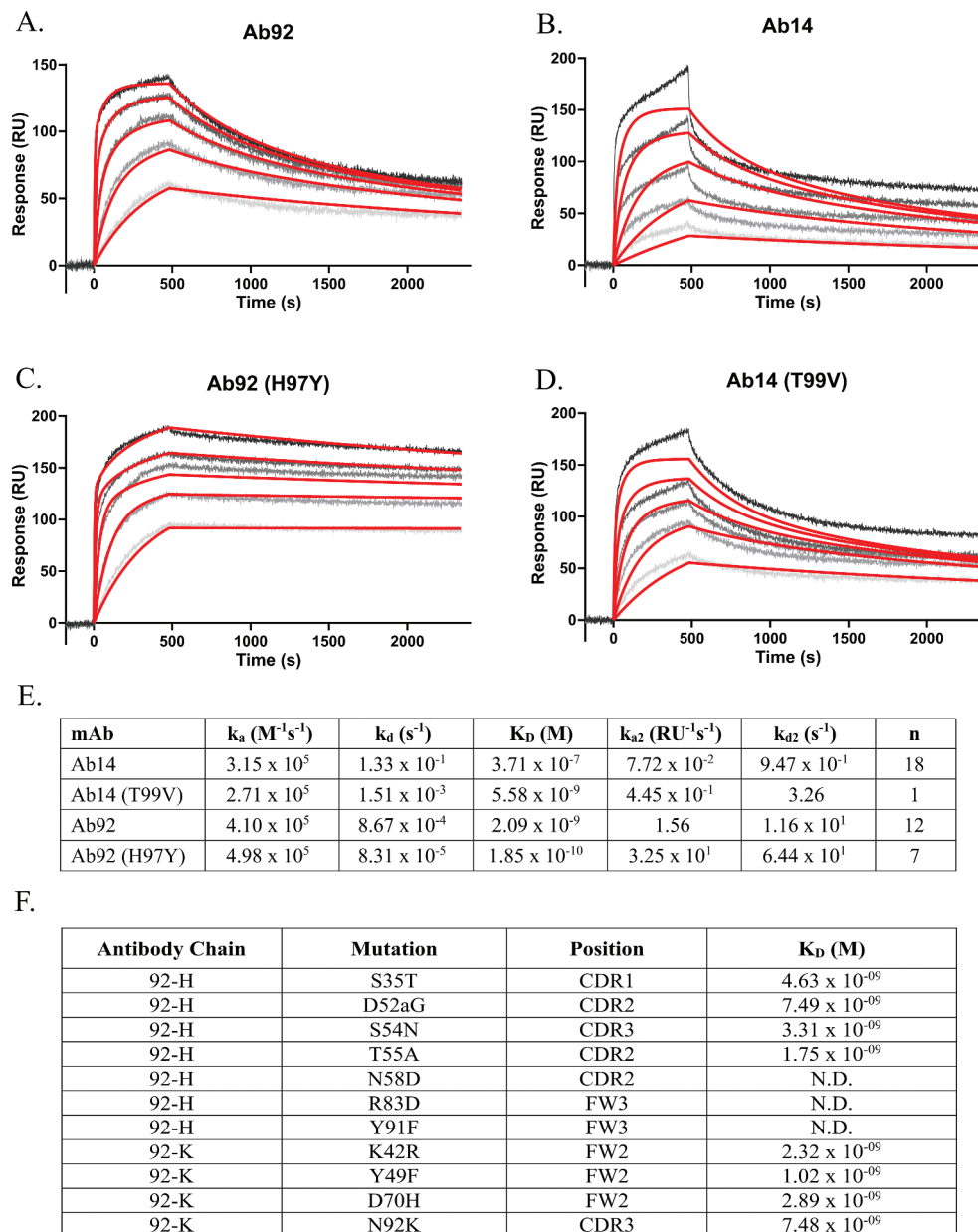


Figure 5. Affinity of parent antibodies to recombinant dimeric HARS(aa1-506) at 150, 50, 16.67, 5.56, and 1.85 nM, fit to bivalent analyte model. Fit lines are displayed in red, experimental data in gray scale. Representative SPR trace of: (a) Ab92, (b) Ab14, (c) Ab92 with H97Y mutation sourced from Ab14, (d) Ab14 with T99V mutation sourced from Ab92. (e) Table of kinetic constants. (f) Summary table of sites of SHM in Ab14 and resulting affinities when transferred to Ab92. Mutations numbered according to Kabat numbering scheme.

prolonged exposure to self-antigen. While it is possible that the extended exposure to antigen in these donors resulted in extensive affinity maturation, SHM rates in the isolated single clones are in fact lower than the general repertoire. It is possible to envision that breaking of immune tolerance in these auto-immune patients results in the generation of highly charged antibodies, escaping traditional checks and balances, and that these are predisposed toward higher affinity without the need for extensive SHM. A third possibility is that high affinity is epitope-dependent, as antibodies to the N- and C-terminal domains were of lower affinity, but those directed to the catalytic domain were frequently of high affinity. Nevertheless, in the analysis of anti-HARS responses, we found sufficient information within the discovered sequences to target further affinity maturation of selected antibodies.

Previous studies looking at responses to vaccination with complex antigens in humans have demonstrated that in some cases, clonal diversity can increase during maturation rather than decrease as a result of clonal competition.^{34,35,45} To utilize this diversity, we recovered a number of related clones from high-throughput single-cell isolation and complementary repertoire sequencing. Initial identification of related clones will, by necessity, be centered on CDR3 homology. However, care must be taken to allow for substitutions maintaining similar characteristics, as the sequence identity of two related clones screened here was quite low (5 of 11 amino acids). It is also possible that the shuffling of light chains and heavy chains done here could also have limitations, as combinations of mutations could potentially sterically compete. Once related clones are identified, it is assumed that at least some of the

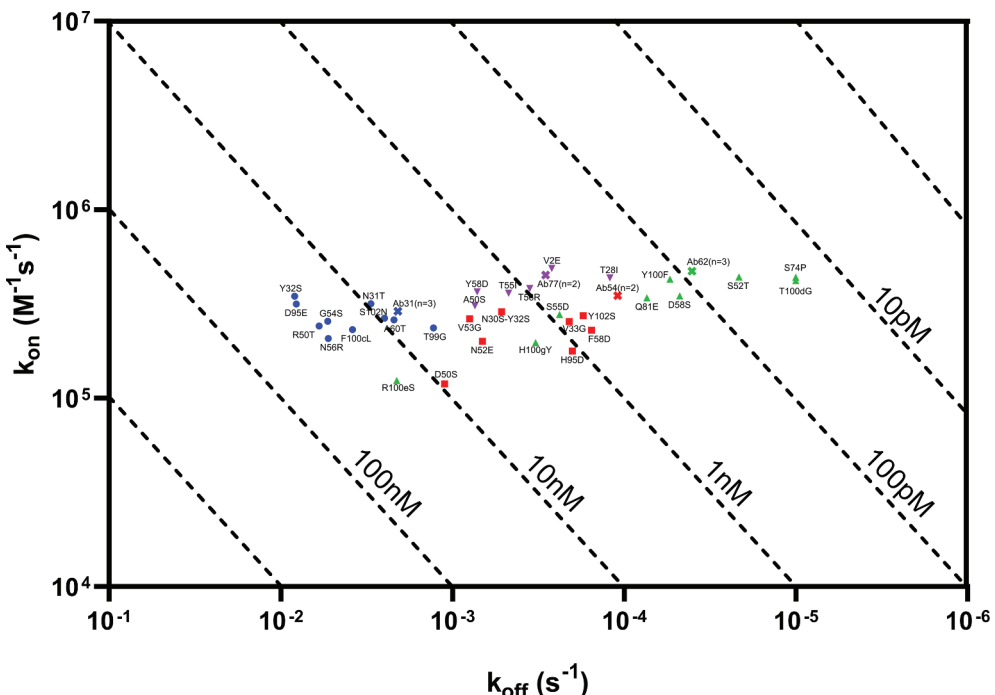


Figure 6. Iso-affinity plot of SHM variants tested for four selected antibodies: Ab31, Ab54, Ab62 and Ab77. Indicated affinities to recombinant dimeric HARS(aa1-506) at 150, 50, 16.67, 5.56, and 1.85 nM, fit to bivalent analyte model. Parent antibodies are displayed as colored crosses, while individual mutants are shown as colored blue circles (Ab31 variants), red squares (Ab54 variants), up green arrows (Ab62 variants) and down purple arrows (Ab77 variants).

affinity-enhancing SHM events in each sequence could highlight residues of importance that present molecular solutions to improved antigen binding, either through direct antigen contact or indirect effects. Given sufficient sequence coverage, analysis of aligned sequences can inform bias for individual substitutions. Convergent mutations would presumably provide strong evidence that a particular pattern is beneficial, whereas highly divergent mutations would suggest the opposite.

It has recently been shown in immunized mice that repertoire derived heavy and light chains can be shuffled into selected antibodies for rapid affinity optimization.⁴⁶ In the case of the Ab14/Ab92 transfer, we saw benefit of mutation transfer from an antibody with sub-optimal heavy and light chains, suggesting that divergent branches can independently discover significant partial solutions, which can be combined to maximize antibody affinity. The two approaches could be used together to further improve affinities beyond that seen with just optimal heavy/light chain pairing, and in fact our initial analysis included chain shuffling between the related recovered clones. The initial mutation transfers between the pair of clonally related WHEP domain binders gave confidence that the direct transfer of mutations from related repertoire sequences would be a viable approach to further the affinity maturation of isolated antigen-specific clones. Computational methods were successful in identifying related sequences that could be used as a source of affinity-enhancing mutations, these mutations were transferred, and showed modest individual benefits. As expected, the lack of preexisting affinity information for these *in silico* isolated sequences did not limit their utility. With minimal effort, equipment, and time, using simple site-directed mutagenesis, a candidate antibody can be

paired with clonally related sequences and at least modestly affinity matured.

While debate continues as to the liabilities of *in vivo*- versus *in vitro*-derived antibodies,^{47,48} developability of protein therapeutics is clearly a current concern in the antibody landscape.⁴⁹⁻⁵¹ As demonstrated in this study, the transfer of selected mutations between isolated B cell clones and from complementary repertoire sequencing data can be used to improve affinity while maintaining *in-vivo* selection. One would assume that this method of affinity maturation can be applied to a number of different approaches, such as antibodies discovered from immunized animals, including transgenic species, as well as from infected, auto-immune, and cancer patients. We have seen similar results transferring mutations between clones from immunized mice (data not shown). While it may be possible to discover pM binders from these platforms, they can be of relatively low frequency compared to the majority of antibodies retrieved,^{42,43} and the best binders may not possess required characteristics such as ligand blocking. In this case, the remainder will often be subjected to some form of *in vitro* affinity maturation. Instead, these selected antibodies can be pooled with related clones from both the initial selection and parallel repertoire sequencing, and matured to higher affinity through a combination of chain swapping and mutation transfer. For those concerned with *in vitro* methods for maturation, these approaches can present an alternative methodology. Such a strategy might be more likely to preserve the desirable characteristics inherent to *in vivo*-derived antibodies. An additional benefit of this method is that residues that would typically be ignored in other rational design approaches (e.g., residues outside CDRs) can be used to further affinity mature antibodies. Two examples in this study are the Ab77-V2E and

the Ab62-S74P mutations. Exploitation of natural SHM events can expand the pool of candidate antibodies while limiting the risks associated with random mutagenesis. Additionally, mutation transfers can be screened for additional desirable properties such as improved developability characteristics.⁵²

The rise of next-generation high-throughput single-cell screening technologies in combination with repertoire sequencing presents a new paradigm for the identification of naturally generated antibodies against any target of interest. Beyond even the approaches discussed here, new approaches enabling massively parallel B-cell sequencing⁵³ as well as connection to antigen reactivity⁵⁴ will continue to increase accessibility to information that can be used to further inform and engineer antibodies of interest.

Materials and methods

Patient selection

Patients were selected based on the following criteria: willing and able to provide written informed consent, between the ages of 18 and 73, with a confirmed clinical diagnosis of any form of myositis, and a confirmed history of a positive anti-Jo-1 antibody titer via medical record review. Patients were excluded due to recent excessive blood loss; known history of HIV, or hepatitis B or C virus infection; pregnancy; history of malignancy; and known positive levels of confounding antibodies. Research protocol was reviewed and approved by the internal institutional review board of Sanguine Biosciences, Study #: SAN-BB-01.

Single-cell isolation

Whole blood was collected from individuals with Jo-1 positive anti-synthetase syndrome under ethical consent. Blood samples were shipped overnight to AbCellera. PBMC isolation and enrichment for plasma cells and B cells using standard protocols (SepMate PBMC isolation protocol, STEMCELL, used as per manufacturer's recommendations) was performed prior to injection into AbCellera's microfluidic screening devices. Single antibody-secreting cells were identified and isolated using AbCellera's microfluidic screening system (U.S. Patent Application No. 14/773,244.)

Single-cell amplification and sequencing

Single-cell PCR and NGS (MiSeq, Illumina) was performed using automated workstations (Bravo, Agilent) and custom molecular biology protocols for the recovery of paired heavy and light chains. Analysis was performed using a custom bioinformatics pipeline to generate a list of paired heavy and light chain antibody sequences. Each sequence was annotated with the closest germline V(D)J gene and degree of SHM. Antibody pairs were considered members of the same clonal group if they shared the same heavy and light V and J genes and had the same CDR3 length.

Repertoire library generation and sequencing

An aliquot of the PBMCs from Donor 1 used in the single-cell screening underwent lysis and PCR to generate a library of repertoire heavy chain sequences. The library was sequenced using two MiSeq 2x300bp runs, generating a total of approximately 37 M paired-end reads. Sequencing data were analyzed using a custom bioinformatics pipeline to generate a list of heavy chain antibody sequences, each annotated with the closest germline V/D/J gene and degree of SHM.

To assemble clonal groups, heavy chain sequences were first clustered according to shared V and J genes and CDR3 length. Single linkage agglomerative hierarchical clustering was then performed using the pairwise "post-normalized Levenshtein" distances between the nucleotide CDR3 sequences within each group.⁵⁵ Next, a fixed distance threshold was determined automatically by analyzing the distance-to-nearest profile for the entire dataset. For each sequence, the distance to its nearest non-identical junction was taken from the complete distance matrix on which the clustering was actually performed. The ideal bandwidth for the kernel density estimate of these distances was then estimated by threefold cross-validation using scikit-learn's model selection package (version 0.21.2). This bandwidth was then used to calculate a binned kernel density estimate of the distances with a Gaussian kernel using scikit-learn's kernel density module. The minima between the two modes of the resulting bimodal distribution was taken as the fixed distance threshold, which was subsequently used to subdivide the distance hierarchies into clonal groups using SciPy's cluster hierarchy package (version 1.3.0).⁵⁶

Plasmid generation and mutagenesis

Antibodies were cloned into expression vectors for heavy chain and light chain (Invivogen, pFUSE-CHIg-hG1 and pFUSE2-CL Ig-hk). Nucleotide sequences of variable regions of antibodies defined by single-cell sequencing were synthesized at GENEWIZ, Inc, and cloned into either pFUSE (heavy chain) using enzyme sites EcoRI and NheI, or pFUSE2 (light chain) using enzyme sites AgeI and BsiWI. Mutations were introduced into plasmids using standard site-directed mutagenesis strategies, using primers with either defined mutations, or NNK oligos targeting individual codons ordered from Integrated DNA Technologies. Primers for mutagenesis were designed using the web-tool available at <https://www.chem.agilent.com/store/primerDesignProgram.jsp>

Transient expression of antibodies

Vectors expressing light chain and heavy chain were cotransfected, typically at a 2:1 mass ratio, into Expi293 cells (ThermoFisher, A14527), grown at 37°C and 8% CO₂. Scale ranged from 400 µl cultures grown in deep-well plates at 350 rpm, to 5 mL cultures grown in 50 mL bioreactors at 215 rpm, to 1 L+ cultures at 125 rpm. 4–5 days post-transfection, when viabilities typically reached <75%, cultures were spun down to remove cell debris and live cells, and supernatants were titered via protein A UPLC, at 215 nm absorbance on an Waters Acuity H Class UPLC against

a standard curve of human IgG (Jackson ImmunoResearch, 009-000-003).

Competition ELISA

Control antibody was biotinylated using EZ-link NSH-PEG₄-Biotin (ThermoFisher, 21363) with a 20-fold molar excess of biotin to IgG. Via an indirect ELISA, biotinylated antibody was titrated against the protein of interest coated at 2 µg/mL in 1x phosphate-buffered saline (PBS) pH 7.4 to determine an appropriate EC50. Competing antibody was diluted by three- or twofold dilutions against control antibody at EC50. All plates were blocked with Casein Blocker (ThermoFisher, 37528), washed with PBST pH 7.4, detected with Streptavidin-HRP (ThermoFisher, SA10001), and developed with TMB Ultra (ThermoFisher, 37574). Data analysis was performed using GraphPad Prism.

Indirect ELISA

Mesoscale Discovery ELISA plates (MSD, L15XA) were coated with target proteins in 1xPBS at 2µg/mL. Antibodies of interest were titrated threefold in 1% BSA/PBS. Plates were blocked with Casein Blocker, washed with PBST pH 7.4, detected with anti-Human-SULFO (MSD, R32AJ) and read in 1x Read buffer (MSD, R92TC) on an MSD QuickPlex. Data analysis was performed using GraphPad Prism.

Binding via Octet-BLI

Binding kinetics of the antibodies were measured on a ForteBio Octet QK 384 instrument using the manufacturer's recommended protocols. Binding assay was performed in ForteBio 1X kinetic buffer. Antibodies were captured on ForteBio kinetic AHC biosensors (ForteBio, 18-5060) at 1 µg/mL and were evaluated for association and dissociation of 100 nM antigen (full-length HARS, WHEP domain-MBP and WHEP domain-deleted HARS). Kinetic binding ranges were derived using ForteBio Octet analysis software.

Binding via ProteOn-SPR

Binding kinetics of the antibodies were measured on a Bio-Rad ProteOn XPR36 Protein Interaction Array instrument. The running buffer for binding experiments was 1x PBS pH 7.4, 0.005% Tween20, and the chip temperature was 25°C. CaptureSelect Human Fab-kappa Kinetics Biotin Conjugate antibody (ThermoFisher, 7103302100) was diluted in running buffer to 15 µg/mL and immobilized on ProteOn NLC sensor chips (Bio-Rad, 1765021). Purified antibody or antibody-containing supernatants were diluted to 0.5 µg/mL antibody concentration in running buffer and captured on the sensor chip by flowing over the anti-human Fab-kappa chip surfaces. Recombinant dimeric HARS (aa1-506) was then flowed in the perpendicular direction, at 150, 50, 16.67, 5.56, and 1.85 nM concentrations. The sensor chip surface was regenerated between each set of antibody supernatants by injections of 10 mM glycine pH 2.0 in both directions. Kinetic binding constants were derived by globally fitting sensograms to a bivalent analyte model (due to the dimeric antigen in use) in the ProteOn Manager software.

Abbreviations

ABD	Anti-codon binding domain
ASS	anti-synthetase syndrome
BLI	bilayer interferometry
CDR	complementarity determining region
ELISA	enzyme-linked immunosorbent assay
FW	framework
HARS	histidyl-tRNA synthetase
Ig	Immunoglobulin
MBP	maltose binding protein
NGS	next generation sequencing
PBMC	peripheral blood mononuclear cells
RT-PCR	reverse transcription polymerase chain reaction
SHM	somatic hypermutation
SPR	surface plasmon resonance
V(D)J	variable(diversity)joining
VH	variable heavy
VK	variable kappa
VL	variable lambda

Acknowledgments

We would like to thank Dr. Andrea Cubitt for helpful discussions regarding the design and implementation of the program, and Dr. Peter Bowers for helpful discussions regarding the clonal analysis of patient data.

Disclosure of potential conflicts of interest

No potential conflicts of interest were disclosed.

References

- Taylor LD, Carmack CE, Schramm SR, Mashayekh R, Higgins KM, Kuo CC, Woodhouse C, Kay RM, Lonberg N. A transgenic mouse that expresses a diversity of human sequence heavy and light chain immunoglobulins. *Nucleic Acids Res.* **1992**;20(23):6287–95. doi:[10.1093/nar/20.23.6287](https://doi.org/10.1093/nar/20.23.6287).
- Kohler G, Milstein C. Continuous cultures of fused cells secreting antibody of predefined specificity. *Nature.* **1975**;256(5517):495–97. doi:[10.1038/256495a0](https://doi.org/10.1038/256495a0).
- McCafferty J, Griffiths AD, Winter G, Chiswell DJ. Phage antibodies: filamentous phage displaying antibody variable domains. *Nature.* **1990**;348:552–54. doi:[10.1038/348552a0](https://doi.org/10.1038/348552a0).
- Boder ET, Wittrup KD. Yeast surface display for screening combinatorial polypeptide libraries. *Nat Biotechnol.* **1997**;15(6):553–57. doi:[10.1038/nbt0697-553](https://doi.org/10.1038/nbt0697-553).
- Higuchi K, Araki T, Matsuzaki O, Sato A, Kanno K, Kitaguchi N, Ito H. Cell display library for gene cloning of variable regions of human antibodies to hepatitis B surface antigen. *J Immunol Methods.* **1997**;202(2):193–204. doi:[10.1016/S0022-1759\(97\)00010-0](https://doi.org/10.1016/S0022-1759(97)00010-0).
- Tiller T, Meffre E, Yurasov S, Tsujii M, Nussenzweig MC, Wardemann H. Efficient generation of monoclonal antibodies from single human B cells by single cell RT-PCR and expression vector cloning. *J Immunol Methods.* **2008**;329:112–24. doi:[10.1016/j.jim.2007.09.017](https://doi.org/10.1016/j.jim.2007.09.017).
- Weinstein JA, Jiang N, White RA, 3rd, Fisher DS, Quake SR. High-throughput sequencing of the zebrafish antibody repertoire. *Science.* **2009**; 324:807–10. doi:[10.1126/science.1170020](https://doi.org/10.1126/science.1170020).
- Jin A, Ozawa T, Tajiri K, Obata T, Kondo S, Kinoshita K, Kadokawa S, Takahashi K, Sugiyama T, Kishi H. A rapid and efficient single-cell manipulation method for screening antigen-specific antibody-secreting cells from human peripheral blood. *Nat Med.* **2009**;15(9):1088–92. doi:[10.1038/nm.1966](https://doi.org/10.1038/nm.1966).
- Corti D, Voss J, Gamblin SJ, Codoni G, Macagno A, Jarrossay D, Vachieri SG, Pinna D, Minola A, Vanzetta F, et al. A neutralizing

- antibody selected from plasma cells that binds to group 1 and group 2 influenza A hemagglutinins. *Science*. 2011;333(6044):850–56. doi:10.1126/science.1205669.
10. Walker LM, Phogat SK, Chan-Hui PY, Wagner D, Phung P, Goss JL, Wrin T, Simek MD, Fling S, Mitcham JL, et al. Broad and potent neutralizing antibodies from an African donor reveal a new HIV-1 vaccine target. *Science*. 2009;326(5950):285–89. doi:10.1126/science.1178746.
 11. Traggiai E, Becker S, Subbarao K, Kolesnikova L, Uematsu Y, Gismondo MR, Murphy BR, Rappuoli R, Lanzavecchia A. An efficient method to make human monoclonal antibodies from memory B cells: potent neutralization of SARS coronavirus. *Nat Med*. 2004;10(8):871–75. doi:10.1038/nm1080.
 12. Scheid JF, Mouquet H, Feldhahn N, Walker BD, Pereyra F, Cutrell E. A method for identification of HIV gp140 binding memory B cells in human blood. *J Immunol Methods*. 2009;343:65–67. doi:10.1016/j.jim.2008.11.012.
 13. Di Niro R, Mesin L, Raki M, Zheng NY, Lund-Johansen F, Lundin KE, Charpilienne A, Poncet D, Wilson PC, Sollid LM. Rapid generation of rotavirus-specific human monoclonal antibodies from small-intestinal mucosa. *J Immunol*. 2010;185(9):5377–83. doi:10.4049/jimmunol.1001587.
 14. DeKosky BJ, Ippolito GC, Deschner RP, Lavinder JJ, Wine Y, Rawlings BM, Varadarajan N, Giesecke C, Dorner T, Andrews SF, et al. High-throughput sequencing of the paired human immunoglobulin heavy and light chain repertoire. *Nat Biotechnol*. 2013;31(2):166–9. doi:10.1038/nbt.2492.
 15. Eyer K, Doineau RCL, Castrillon CE, Briseno-Roa L, Menrath V, Mottet G, England P, Godina A, Brent-Litzler E, Nizak C, et al. Single-cell deep phenotyping of IgG-secreting cells for high-resolution immune monitoring. *Nat Biotechnol*. 2017;35(10):977–82. doi:10.1038/nbt.3964.
 16. Georgiou G, Ippolito GC, Beausang J, Busse CE, Wardemann H, Quake SR. The promise and challenge of high-throughput sequencing of the antibody repertoire. *Nat Biotechnol*. 2014;32:158–68. doi:10.1038/nbt.2782.
 17. DeKosky BJ, Kojima T, Rodin A, Charab W, Ippolito GC, Ellington AD, Georgiou G. In-depth determination and analysis of the human paired heavy- and light-chain antibody repertoire. *Nat Med*. 2015;21(1):86–91. doi:10.1038/nm.3743.
 18. Fonville JM, Wilks SH, James SL, Fox A, Ventresca M, Aban M, Xue L, Jones TC, Le NM, Pham QT, Tran ND. Antibody landscapes after influenza virus infection or vaccination. *Science*. 2014;346(6212):996–1000. doi:10.1126/science.1256427.
 19. DeKosky BJ, Lungu OI, Park D, Johnson EL, Charab W, Chrysostomou C, Kuroda D, Ellington AD, Ippolito GC, Gray JJ, et al. Large-scale sequence and structural comparisons of human naïve and antigen-experienced antibody repertoires. *Proc Natl Acad Sci U S A*. 2016;113(19):E2636–45. doi:10.1073/pnas.1525510113.
 20. Hersberg U, Luning Prak ET. The analysis of clonal expansions in normal and autoimmune B cell repertoires. *Philosophical Transactions of the Royal Society B: Biological Sciences*. 2015;370(1676):20140239. doi:10.1098/rstb.2014.0239.
 21. de Bourcy CF, Angel CJ, Vollmers C, Dekker CL, Davis MM, Quake SR. Phylogenetic analysis of the human antibody repertoire reveals quantitative signatures of immune senescence and aging. *Proc Natl Acad Sci U S A*. 2017;114(5):1105–10. doi:10.1073/pnas.1617959114.
 22. Johnson EL, Doria-Rose NA, Gorman J, Bhiman JN, Schramm CA, Vu AQ, Law WH, Zhang B, Bekker V, Abdool Karim SS, et al. Sequencing HIV-neutralizing antibody exons and introns reveals detailed aspects of lineage maturation. *Nat Commun*. 2018;9(1):4136. doi:10.1038/s41467-018-06424-6.
 23. Lo WS, Gardiner E, Xu Z, Lau CF, Wang F, Zhou JJ, Mendlein JD, Nangle LA, Chiang KP, Yang X-L, et al. Human tRNA synthetase catalytic nulls with diverse functions. *Science*. 2014;345(6194):328–32. doi:10.1126/science.1252943.
 24. Kanaji T, Vo MN, Kanaji S, Zarpellon A, Shapiro R, Morodomi Y, Yuzurihara A, Eto K, Belani R, Do M-H, et al. Tyrosyl-tRNA synthetase stimulates thrombopoietin-independent hematopoiesis accelerating recovery from thrombocytopenia. *Proc Natl Acad Sci U S A*. 2018;115(35):E8228–E35. doi:10.1073/pnas.1807000115.
 25. Xu X, Shi Y, Zhang HM, Swindell EC, Marshall AG, Guo M, Kishi S, Yang X-L. Unique domain appended to vertebrate tRNA synthetase is essential for vascular development. *Nat Commun*. 2012;3(1):681. doi:10.1038/ncomms1686.
 26. Zhou JJ, Wang F, Xu Z, Lo WS, Lau CF, Chiang KP, Nangle LA, Ashlock MA, Mendlein JD, Yang X-L. Secreted histidyl-tRNA synthetase splice variants elaborate major epitopes for autoantibodies in inflammatory myositis. *J Biol Chem*. 2014;289(28):19269–75. doi:10.1074/jbc.C114.571026.
 27. Kron MA, Metwali A, Vodanovic-Jankovic S, Elliott D. Nematode asparaginyl-tRNA synthetase resolves intestinal inflammation in mice with T-cell transfer colitis. *Clin vaccine immunol*. 2013;20(2):276–81. doi:10.1128/CVI.00594-12.
 28. Kim SB, Kim HR, Park MC, Cho S, Goughnour PC, Han D, Yoon I, Kim Y, Kang T, Song E, et al. Caspase-8 controls the secretion of inflammatory lysyl-tRNA synthetase in exosomes from cancer cells. *J Cell Biol*. 2017;216(7):2201–16. doi:10.1083/jcb.201605118.
 29. Adams RA, Fernandes-Cerdeira C, Notaricola A, Mertsching E, Xu Z, Lo WS, Ogilvie K, Chiang KP, Ampudia J, Rosengren S, et al. Serum-circulating His-tRNA synthetase inhibits organ-targeted immune responses. *Cell Mol Immunol*. 2019. doi:10.1038/s41423-019-0331-0.
 30. Mathews MB, Bernstein RM. Myositis autoantibody inhibits histidyl-tRNA synthetase: a model for autoimmunity. *Nature*. 1983;304(5922):177–79. doi:10.1038/304177a0.
 31. Fitzgerald V, Leonard P. Single cell screening approaches for antibody discovery. *Methods*. 2017;116:34–42. doi:10.1016/j.ymeth.2016.11.006.
 32. Mahler M, Miller FW, Fritzler MJ. Idiopathic inflammatory myopathies and the anti-synthetase syndrome: A comprehensive review. *Autoimmun Rev*. 2014;13(4–5):367–71. doi:10.1016/j.autrev.2014.01.022.
 33. Svensson J, Arkema EV, Lundberg IE, Holmqvist M. Incidence and prevalence of idiopathic inflammatory myopathies in Sweden: a nationwide population-based study. *Rheumatology (Oxford)*. 2017;56(5):802–10. doi:10.1093/rheumatology/kew503.
 34. Kuraoka M, Schmidt AG, Nojima T, Feng F, Watanabe A, Kitamura D, et al. Complex antigens drive permissive clonal selection in germinal centers. *Immunity*. 2016;44:542–52. doi:10.1016/j.immuni.2016.02.010.
 35. Khavrutskii IV, Chaudhury S, Stronsky SM, Lee DW, Benko JG, Wallqvist A, Bavari S, Cooper CL. Quantitative Analysis of Repertoire-Scale Immunoglobulin Properties in Vaccine-Induced B-Cell Responses. *Front Immunol*. 2017;8:910. doi:10.3389/fimmu.2017.00910.
 36. Shugay M, Britanova OV, Merzlyak EM, Turchaninova MA, Mamedov IZ, Tuganbaev TR, Bolotin DA, Staroverov DB, Putintseva EV, Plevova K. Towards error-free profiling of immune repertoires. *Nat Methods*. 2014;11(6):653–55. doi:10.1038/nmeth.2960.
 37. Yaari G, Kleinsteiner SH. Practical guidelines for B-cell receptor repertoire sequencing analysis. *Genome Med*. 2015;7:121. doi:10.1186/s13073-015-0243-2.
 38. Kitaura K, Yamashita H, Ayabe H, Shini T, Matsutani T, Suzuki R. Different somatic hypermutation levels among antibody subclasses disclosed by a new next-generation sequencing-based antibody repertoire analysis. *Front Immunol*. 2017;8:389. doi:10.3389/fimmu.2017.00389.
 39. Wardemann H, Yurasov S, Schaefer A, Young JW, Meffre E, Nussenzweig MC. Predominant autoantibody production by early human B cell precursors. *Science*. 2003;301(5638):1374–77. doi:10.1126/science.1086907.
 40. Xu Z, Wei Z, Zhou JJ, Ye F, Lo WS, Wang F, Lau C-F, Wu J, Nangle L, Chiang K, et al. Internally deleted human tRNA synthetase suggests evolutionary pressure for repurposing. *Structure*. 2012;20(9):1470–77. doi:10.1016/j.str.2012.08.001.
 41. Alam ME, Geng SB, Bender C, Ludwig SD, Linden L, Hoet R, Tessier PM. Biophysical and sequence-based methods for

- identifying monovalent and bivalent antibodies with high colloidal stability. *Mol Pharm*. 2018;15(1):150–63. doi:10.1021/acs.molpharmaceut.7b00779.
42. Batista FD, Neuberger MS. Affinity dependence of the B cell response to antigen: a threshold, a ceiling, and the importance of off-rate. *Immunity*. 1998;8(6):751–59. doi:10.1016/S1074-7613(00)80580-4.
 43. Foote J, Eisen HN. Kinetic and affinity limits on antibodies produced during immune responses. *Proc Natl Acad Sci U S A*. 1995;92(5):1254–56. doi:10.1073/pnas.92.5.1254.
 44. Poulsen TR, Jensen A, Haurum JS, Andersen PS. Limits for antibody affinity maturation and repertoire diversification in hyper-vaccinated humans. *J Immunol*. 2011;187(8):4229–35. doi:10.4049/jimmunol.1000928.
 45. Victora GD, Wilson PC. Germinal center selection and the antibody response to influenza. *Cell*. 2015;163(3):545–48. doi:10.1016/j.cell.2015.10.004.
 46. Hsiao YC, Shang Y, DiCara DM, Yee A, Lai J, Kim SH, Ellerman D, Corpuz R, Chen Y, Rajan S. Immune repertoire mining for rapid affinity optimization of mouse monoclonal antibodies. *mAbs*. 2019;11(4):735–46. doi:10.1080/19420862.2019.1584517.
 47. Nixon AE, Sexton DJ, Ladner RC. Drugs derived from phage display: from candidate identification to clinical practice. *mAbs*. 2014;6(1):73–85. doi:10.4161/mabs.27240.
 48. Spencer S, Bethea D, Raju TS, Giles-Komar J, Feng Y. Solubility evaluation of murine hybridoma antibodies. *mAbs*. 2012;4(3):319–25. doi:10.4161/mabs.19869.
 49. Jain T, Sun T, Durand S, Hall A, Houston NR, Nett JH, Sharkey B, Bobrowicz B, Caffry I, Yu Y, et al. Biophysical properties of the clinical-stage antibody landscape. *Proc Natl Acad Sci U S A*. 2017;114(5):944–49. doi:10.1073/pnas.1616408114.
 50. Xu Y, Roach W, Sun T, Jain T, Prinz B, Yu TY, Torrey J, Thomas J, Bobrowicz P, Vasquez M, et al. Addressing polyspecificity of antibodies selected from an in vitro yeast presentation system: a FACS-based, high-throughput selection and analytical tool. *Protein Engineering Design and Selection*. 2013;26(10):663–70. doi:10.1093/protein/gzt047.
 51. Avery LB, Wade J, Wang M, Tam A, King A, Piche-Nicholas N, Kavosi MS, Penn S, Cirelli D, Kurz JC, et al. Establishing in vitro in vivo correlations to screen monoclonal antibodies for physico-chemical properties related to favorable human pharmacokinetics. *mAbs*. 2018;10(2):244–55. doi:10.1080/19420862.2017.1417718.
 52. Wang F, Sen S, Zhang Y, Ahmad I, Zhu X, Wilson IA, Smider VV, Magliery TJ, Schultz PG. Somatic hypermutation maintains antibody thermodynamic stability during affinity maturation. *Proc Natl Acad Sci U S A*. 2013;110(11):4261–66. doi:10.1073/pnas.1301810110.
 53. Goldstein LD, Chen YJ, Wu J, Chaudhuri S, Hsiao YC, Schneider K, Hoi KH, Lin Z, Guerrero S, Jaiswal BS. Massively parallel single-cell B-cell receptor sequencing enables rapid discovery of diverse antigen-reactive antibodies. *Commun Biol*. 2019;2(1):304. doi:10.1038/s42003-019-0551-y.
 54. Setliff I, Shiakolas AR, Pilewski KA, Murji AA, Mapengo RE, Janowska K, Richardson S, Oosthuysen C, Raju N, Ronsard L, et al. High-throughput mapping of B cell receptor sequences to antigen specificity. *Cell*. 2019;179(7):1636–46 e15. doi:10.1016/j.cell.2019.11.003.
 55. Chen Z, Collins AM, Wang Y, Gaeta BA. Clustering-based identification of clonally-related immunoglobulin gene sequence sets. *Immunome Res*. 2010;6(Suppl 1):S4. doi:10.1186/1745-7580-6-S1-S4.
 56. Gupta NT, Adams KD, Briggs AW, Timberlake SC, Vigneault F, Kleinstein SH. Hierarchical clustering can identify B cell clones with high confidence in Ig repertoire sequencing data. *J Immunol*. 2017;198(6):2489–99. doi:10.4049/jimmunol.1601850.